High-Potency Polypeptide-based Interference for Coronavirus Spike Glycoproteins

Jianpeng Ma[1,2,*], Adam Campos Acevedo[2], and Qinghua Wang[2,*]

[1]Multiscale Research Institute for Complex Systems, Fudan University, 653 Huatuo Road, Shanghai, 201203, China; [2]Verna and Marrs McLean Department of Biochemistry and Molecular Biology, Baylor College of Medicine, One Baylor Plaza, Houston, TX 77030, USA

[*]Corresponding authors: Qinghua Wang (Email: qinghuaw@bcm.edu, Phone: 713-798-5289) and Jianpeng Ma (Email: jpma@bcm.edu, Phone: 713-798-8187).

April 2, 2021

Running Title: Inhibiting coronavirus spike proteins

Keywords: Coronavirus, COVID-19, inhibitor, SARS-CoV-2, spike glycoproteins

Abstract

The world is experiencing an unprecedented coronavirus disease 2019 (COVID-19) pandemic caused by severe acute respiratory syndrome coronavirus 2 (SARS-CoV-2). SARS-CoV-2 spike protein-based vaccines are currently the main preventive agent to fight against the virus. However, several variants with extensive mutations in SARS-CoV-2 spike proteins have emerged. Some of these variants exhibited increased replication, higher transmission and virulence, and were partially resistant to antibody neutralization from natural infection or vaccination. With over 130 million confirmed cases and widespread vaccination around the globe, the emergence of new escape SARS-CoV-2 variants could be accelerated. New therapeutics insensitive to mutations are thus urgently needed. Here we have developed an inhibitor based on SARS-CoV-2 spike protein that potently reduced pseudovirus infectivity by limiting the level of SARS-CoV-2 spike proteins on virion envelope. Most importantly, the inhibitor was equally effective against other coronavirus spike proteins that shared as low as 35% amino-acid sequence identity, underscoring its extreme tolerance to mutations. The small-sized inhibitor would also allow simple delivery by, for instance, nasal spray. We expect the inhibitor reported here to be an invaluable aid to help end COVID-19 pandemic. Furthermore, the use of a partial native sequence or its homologues to interfere with the functions of the native protein represents a novel concept for targeting other viral proteins in combating against important viral pathogens.

Main text

In the past 20 years, there have been three major threats from coronavirus, the 2002-2003 outbreak in China from severe acute respiratory syndrome coronavirus (SARS-CoV), the 2012-2014 outbreak in Middle East from Middle East respiratory syndrome coronavirus (MERS-CoV)[1,2], and the ongoing COVID-19 pandemic caused by SARS-CoV-2. Currently, the world is racing to contain

SARS-CoV-2 mainly by using SARS-CoV-2 spike protein (SARS2-S)-based vaccines. However, continued genomic evolution has led to SARS-CoV-2 variants with extensive mutations on SARS2-S proteins[3-5] **(Fig.1a)**. These mutations endorsed tighter binding with host cell surface receptor, human angiotensin-converting enzyme 2 (hACE2), higher virulence, resistance to antibody neutralization and escape from natural infection or vaccine induced sera[6-10]. Therefore, there is an urgent need for other interventions that are insensitive to genomic mutations.

Towards this end, we have developed a polypeptide-based inhibitor, F1, that potently interfered with the formation and translocation of coronavirus spike glycoproteins to host cell surface and to the envelope of generated pseudoviruses. Although derived from the SARS2-S sequence, F1 was also effective on 2002 SARS-CoV spike protein (SARS-S) and 2012 MERS-CoV spike protein (MERS-S). These sequences shared as low as 35% amino-acid sequence identity, stressing the extreme resistance of F1 to mutations in spike sequences of emerging COVID-19 SARS-CoV-2 variants. Different from traditional protein-based therapeutics, the F1 polypeptide-based interference requires that the plasmid or minicircle DNA harboring F1-coding gene is delivered into the host to synthesize F1 polypeptide at the site where the target spike proteins are synthesized. Therefore, the rapid degradation intrinsically associated with protein/polypeptide-based therapeutics is no longer a problem. Moreover, the small-sized F1-minicircle developed here would also allow simple delivery by, for example, nasal spray. We expect the inhibitor reported here to be an invaluable aid to our effort to stop COVID-19 pandemic.

The concept of polypeptide-based protein interference

Viral membrane fusion proteins such as coronavirus spike proteins are oligomeric Class-I transmembrane glycoproteins on the viral envelope[11]. Coronavirus spike proteins are cleaved to give rise to N-terminal S1 regions and C-terminal S2 regions (**Fig.1a**). The N-terminal S1 regions are the

major target for neutralizing antibodies elicited by natural infection or vaccination, and therefore under constant positive selection for escape variants (**Fig.1a**). On the other hand, the C-terminal S2 regions responsible for oligomerization and membrane fusion[12-16] are more conserved among different coronavirus strains. Upon entry into a host cell, the viral genome will guide the synthesis of new coronavirus spike proteins by ribosomes, which are then folded, assembled and translocated into endoplasmic reticulum (ER) membranes and transit through the ER-to-Golgi intermediate compartment for interaction with newly replicated genomic RNA to produce new virions[17,18].

We hypothesized that stably foldable fragments of the coronavirus spike proteins, for instance, polypeptides derived from the SARS2-S S2 regions, which maintained the same oligomeric interface as the native spike proteins, would form non-native oligomers with the wild-type spike proteins, thus significantly lowering the level of native spike oligomers on the envelope of newly generated virions, and impairing their infectivity (**Fig.1b**). More importantly, the fragment derived from the conserved S2 region would be more resistant to mutations and could be potentially "universal" against different coronaviruses. To test this strategy, we made two polypeptides derived from the SARS2-S sequence, F1 and F2, that contained partial SARS2-S S2 sequence (**Fig.1a, Fig.S1, S2**). F1 polypeptide encompassed amino-acid residues 911~1273, while F2 harbored residues 985~1273. Both polypeptides contained a N-terminal signal peptide (SP) as the wild-type SARS2-S for cell surface translocation.

F1 polypeptide potently inhibited expression and cell surface translocation of multiple coronavirus spike glycoproteins

We first assessed the impacts of F1 or F2 on the expression and cell surface translocation of SARS2-S protein. Transient transfection of SARS2-S-harboring plasmid yielded a good level of proteins detected in HEK293T whole cell lysate, with most of the expressed proteins were cleaved

(**Fig.2a**). This high-efficiency cleavage of SARS2-S proteins agreed with the novel polybasic cleavage site at the S1/S2 boundary[12,13,19,20]. Moreover, only the S2 fragments of the cleaved SARS2-S protein were labeled by biotin, affinity-purified by anti-biotin antibody and detected in cell surface fraction (**Fig.2a**), suggesting that only properly cleaved SARS2-S protein were translocated to cell surface. Most impressively, when F1-harboring plasmid was co-transfected with SARS2-S-carrying plasmid, even at a twofold molar ratio, the predominant cleaved S2 band of SARS2-S was almost completely diminished in whole cell lysate and in cell surface fraction (**Fig.2a**). Thus, F1 strongly interfered with the expression and cell surface translocation of SARS2-S. In sharp contrast, F2 did not exhibit any significant interference even at a tenfold molar ratio (**Fig.2a**).

Sequence comparison of 2002 SARS-S, 2012 MERS-S and COVID-19 SARS2-S suggested a wide range of sequence identity levels among them (**Fig.S2, S3**). For instance, 2002 SARS-S shared 77% amino-acid sequence identity with full-length COVID-19 SARS2-S, while 2012 MERS-S was only at 35% (**Fig.S2, S3**). If only considering the regions included in F1 polypeptide, the identical residues became 94% for 2002 SARS-S and 42% for 2012 MERS-S (**Fig.S2, S3**). These spike proteins with a wide range of sequence identity levels were ideal for testing the insensitivity of F1-induced interference to amino-acid changes. Strikingly, even with F1-harboring plasmid at a twofold molar ratio, the cleaved SARS-S and MERS-S S2 bands were almost completely diminished in whole cell lysate and in cell surface fraction (**Fig.2b,c**). Thus, despite the low sequence identity, F1 also strongly interfered with the expression and cell surface translocation of SARS-S and MERS-S glycoproteins. Consistent with the robust interference activity exhibited by F1 (**Fig.2**), a high level of F1 polypeptide was constantly detected in cell surface fraction (**Fig.S4a-c**). In marked contrast, a limited level of F2 polypeptide was detected in cell surface fraction (**Fig.S4a**), in agreement with the non-interference of F2 (**Fig.2a**).

F1 interfered with coronavirus spike proteins at the protein level

In order to probe the mechanism of F1-mediated interference of coronavirus spike proteins, we analyzed the mRNA levels of coronavirus spike proteins in the absence or presence of F1 or F2-carrying plasmids (**Fig.S5, S6**). Clearly co-transfection of F1- or F2-harboring plasmids did not significantly change the mRNA levels of coronavirus spike proteins, which were kept at a relatively constant level (between 50%~150%) comparing to the samples that were transfected only with plasmids carrying the respective coronavirus spike gene (**Fig.S5**). In sharp contrast, the mRNA levels of F1 were at the order of 2^6.5~2^12 when normalized against endogenous GAPDH (**Fig.S6**), justifying the high potency of F1-mediated interference. The mRNA levels of F2 were comparable with those of F1 (**Fig.S6a**), in marked contrast with the low level of F2 polypeptide detected in cell surface fraction (**Fig.S4a**), suggested that the non-interference of F2 (**Fig.2a**) was likely due to the instability of the synthesized F2 polypeptide. Collectively, these data suggested that F1-mediated interference of various coronavirus spike glycoproteins was not at the mRNA level.

We next investigated whether SARS2-S and F1 directly interacted with each other to form non-native oligomers in the cell. SARS2-S and F1 were each tagged with a monomeric green fluorescent protein (GFP) variant at the extreme C-terminus, CFP for SARS2-S (termed as SARS2C) and YFP for F1 (named as F1Y) (**Fig.S5d**). Since the expression of SARS2-S was completely diminished when F1- and SARS2-S-carrying plasmids were co-transfected at a 2:1 molar ratio (**Fig.2a**), we used F1Y- and SARS2C-containing plasmids at a reduced 1:1 molar ratio to transiently transfect HEK293T cells, and monitored fluorescence resonance energy transfer (FRET) between them. The FRET ratio (FR) was determined by using the three-cube approach[21]. Although the non-native oligomers formed by SRARS2C and F1Y were expected to be highly unstable, FRET signals between them were robustly detected (**Fig.S5e**), supporting direct interactions between SARS2-S and F1. Collectively, these results

suggested that F1-mediated interference of various coronavirus spike glycoproteins was at the protein level.

F1 minicircle potently interfered with expression and cell surface translocation of all three coronavirus spike glycoproteins

The high potency of F1 in interfering with expression and surface translocation of the spike glycoproteins from coronaviruses that caused severe outbreaks or pandemic between 2002 to 2021 suggests that F1 has a high promise to become an effective therapeutic agent against different coronavirus lineages over a long time period. Therefore, we sought to identify a convenient way to deliver F1 for therapeutic purpose. The potent interference activity of F1 requires it to co-localize with its target spike protein at the time of protein synthesis, therefore F1-encoding gene needs to be delivered to the site of action. Minicircles are a type of newly developed DNA carriers for gene therapy[22]. The main features of minicircles include the cleaner gene background with minimal viral or bacterial gene elements, sustained high-level protein expression, and more importantly, the small size that may allow the use of aerosols for drug delivery[23]. The latter may be a distinct advantage against coronavirus-caused respiratory diseases.

We made a F1 minicircle by inserting the F1 coding sequence into the parental minicircle cloning vector pMC.CMV-MCS-SV40polyA (**Fig.3a**), and tested its efficacy in interfering with expression and surface translocation of coronavirus spike glycoproteins. Compared to the controls where no minicircle was used, the presence of F1 minicircles, at a merely 4.5-fold molar ratio, almost completely abolished cell surface translocation of all three spike proteins (**Fig.3b-d**). It is important to emphasis that this level of potent interference was achieved under the situation where pcDNA3.1-based plasmids harboring coronavirus spike-coding genes were efficiently replicated in HEK293T cells, while

F1 minicircle cannot. Therefore, F1 minicircle demonstrated strong interference with the expression and cell surface translocation of these coronavirus spike proteins.

F1 minicircle reduced the level of SARS2-S protein on intact pseudoviruses and impaired pseudovirus infectivity

To investigate the consequences of the reduced cell surface translocation of coronavirus spike proteins by F1 minicircle, we compared the level of SARS2-S protein on pseudoviruses generated using luciferase-expressing, *env*-defective HIV-1 genome plasmid pRL4.3-Luc-R^-E^- in the presence of different molar ratios of control minicircle made from the empty parental vector (termed as MN501A) or F1 minicircle. In order to make sure that only spike proteins anchored on the pseudovirus envelope were accounted for, we employed QuickTiter Lentivirus Titer kit to precipitate intact pseudoviruses from cleared supernatant prior to analysis by western blot. Impressively, even with a twofold molar ratio of F1 minicircle, almost no SARS2-S was detected on the generated intact pseudoviruses (**Fig.4a**). Not surprisingly, these pseudoviruses completely failed to infect hACE2-expressing HEK293T cells (**Fig.4b**).

Discussion

In the current research, we present a series of compelling evidence that the F1 polypeptide derived from COVID-19 SARS2-S potently reduced the expression and surface translocation of the spike proteins from all three coronaviruses that caused regional outbreaks or global pandemic in the last 20 years, despite as low as 35% amino-acid sequence identity among them. Although extensive mutations were found on SARS2-S proteins in recent SARS-CoV-2 variants[3-5] (**Fig.1a**), the regions corresponding to F1 polypeptide were highly conserved, as exemplified by the nearly identical sequence of SARS-CoV-2 B.1.1.7-S with F1 (**Fig.S3b**). Therefore, F1 polypeptide is expected to be effective on

the spike proteins of almost any emerging COVID-19 SARS-CoV-2 variants in the future. Furthermore, since the spike proteins of other human coronaviruses and 2012 MERS-CoV have a similar level of sequence identity with F1 (**Fig.S3b**), we expect F1 to be equally effective on all these spike proteins. Moreover, this polypeptide-based interference targeting the conserved sequences of coronavirus spike protein to interfere with its functions represents a novel concept for therapeutics with high efficacy and specificity, resistance to evolution and easy adaptability to other viral proteins in combating against important viral pathogens.

Figure captions

Figure 1. The concept of polypeptide-based protein interference against coronavirus spike proteins. a). Domain organization of COVID-19 SARS2-S**,** the mutations in recent variants and the design of interfering polypeptides F1 and F2. SP: Signal peptide; NTD: N-terminal domain; RBD: receptor-binding domain; SD1: subdomain 1; SD2: subdomain 2; FP: fusion peptide; HR1: heptad repeat 1; HR2: heptad repeat 2; TM: transmembrane domain; CT: Cytoplasmic tail. The cleavage at S1/S2 (red arrow) gives rise to N-terminal S1 fragment and C-terminal S2 fragment. The signal peptide sequence at the extreme N-termini of F1 and F2 allowed the polypeptides to be translocated in the same way as COVID-19 SARS2-S. At the extreme C-termini, SARS2-S had a C9 epitope recognized by C9-rhodopsin antibody 1D4, while both F1 and F2 had a FLAG-tag. **b).** Diagram of polypeptide-based interference targeting coronavirus spike proteins. Top row: in the normal situation, the spike proteins were synthesized, folded and formed native spike oligomers, which were anchored on virion envelope. Bottom row, interfering polypeptides formed non-native oligomers with the wild-type spike proteins, thus reducing the level of native spike oligomers on the envelope of new virions.

Figure 2. F1 significantly reduced expression and surface translocation of three coronavirus spike glycoproteins. **a).** COVID-19 SARS2-S. **b).** 2002 SARS-S. **c).** 2012 MERS-S. For panels **a-c)**, the levels of S protein in whole cell lysate (left) or in cell surface fraction (right) were compared for HEK293T cells transfected with S-containing plasmid only (Sample 1), or together with twofold (Sample 2) or tenfold molar ratio (Sample 3) of F1-containing plasmid, and in panel **a)** with twofold (Sample 4) or tenfold molar ratio (Sample 5) of F2-containing plasmid.

Figure 3. F1 minicircle significantly reduced expression and surface translocation of three coronavirus spike glycoproteins. **a).** Diagram for the production of F1 minicircle used in this study. **b).** COVID-19 SARS2-S; **c).** 2002 SARS-S; **d).** 2012 MERS-S. The levels of uncleaved S protein and the cleaved S2 protein in whole cell lysate (left) or in cell surface fraction (right) were compared for HEK293T cells transfected with S-containing plasmid only (Sample 1), or together with 4.5-fold (Sample 2) or 22.5-fold molar ratio (Sample 3) of F1 minicircles.

Figure 4. F1 minicircle significantly reduced the level of SARS2-S on intact pseudoviruses and impaired pseudovirus infectivity. **a).** The level of cleaved S2 protein was compared for intact pseudovirus produced from HEK293T cells transfected with SARS2-S-containing plasmid and different ratios of empty minicircle control, MN501A (Sample 1~4), or F1 minicircle (Sample 5~8). **b).** Pseudovirus generated in the presence of F1 minicircle at a twofold molar ratio completely lost the ability to infect hACE2-expressing HEK293T cells. The infectivity of pseudovirus generated in the presence of MN501A minicircle at a twofold molar ratio was considered as 100%.

Materials and Methods

Materials

The pcDNA3.1 plasmids harboring the genes encoding SARS-CoV spike (GenBank accession number AFR58740.1), SARS-CoV-2 spike (GenBank accession number QHD43416.1), and human ACE2 (GenBank accession number NM_021804) were kind gifts from Dr. Fang Li[14] (Addgene plasmid No. 145031, 145032 and 145033, respectively). The pcDNA3.1 plasmids harboring the genes encoding MERS-CoV spike (GenBank accession number QBM11748.1), F1 or F2 polypeptides were synthesized by Genscript Biotech (Piscataway, NJ, USA). The parental minicircle vector pMC.CMV-MCS-SV40polyA (Cat. No. MN501A-1), ZYCY10P3S2T *E. coli* minicircle producer strain[24] competent cells (Cat. No. MN900A-1) and Arabinose Induction Solution (Cat. No. MN850A-1) were purchased from System Biosciences (Palo Alto, CA, USA). The luciferase-expressing, *env*-defective HIV-1 genome plasmid pRL4.3-Luc-R^-E^- (Cat. No. 3418) was obtained through the NIH AIDS Reagent Program, Division of AIDS, NIAID, NIH, USA. C9-rhodopsin antibody 1D4 HRP (Cat. No. sc57432 HRP) and 2',3'-cyclinc nucleotide 3'-phosphodiesterase (CNPase) antibody (Cat. No. A01308) were purchased from Santa Cruz Biotechnology, Inc. (Dallas, TX, USA) and Genscript Biotech (Piscataway, NJ, USA), respectively. QuickTiter Lentivirus Titer kit (Cat. No. VPK-107) was purchased from Cell Biolabs Inc (San Diego, CA, USA). Pierce Cell surface Protein Biotinylation and Isolation Kit (Cat. No. A44390) was purchased from Thermo Scientific, Waltham, MA, USA. Quick-RNA miniprep Kit (Cat. No. R1054) and ZymoPURE II Plasmid Maxiprep Kit (Cat. No. D4203) were obtained from Zymo Research, Irvine, CA, USA. iScript Reverse Transcription Supermix (Cat. No. 1708840) was purchased from Bio-rad, Hercules, CA, USA. Bimake SYBR Green qPCR Master Mix (Cat. No. B21203) was obtained from Bimake, Houston, TX, USA. Lipofectine 3000 (Cat. No. L3000015) was obtained from Invitrogen, Carlsbad, CA, USA. One-Glo EX Luciferase Assay System (Cat. No. E8110) was purchased from Promega, Madison, WI, USA. HEK293T cells (Cat. No. CRL-11268) were purchased from American

Type Culture Collection (Manassas, VA, USA) and maintained in DMEM medium containing 10% fetal bovine serum (FBS) at 37°C incubator supplied with 5% CO2.

Cell surface biotinylation and protein purification

Cell surface biotinylation and protein purification were performed using Pierce Cell surface Protein Biotinylation and Isolation Kit following the manufacturer's instruction. Briefly, cell surface proteins on HEK293T cells were first labeled with Sulfo-NHS-SS-Biotin at 4°C for 30 minutes, which were then stopped by adding Tris-buffered saline and further washed. After cells were lysed with Lysis Buffer, lysate was cleared by centrifugation. Cleared lysate was incubated with NeutrAvidin Agarose to allow binding of biotinylated proteins. After extensive wash, the bound proteins were eluted with Elution Buffer containing 10 mM DTT. The cleared lysate ("Whole cell" fraction) and eluted proteins ("Cell surface" fraction) were run on 10% SDS-PAGE and the spike proteins were detected by C9-rhodopsin antibody 1D4 HRP. Endogenous membrane-anchored protein CNPase was detected by anti-CNPase antibody and served as an internal control.

Total RNA isolation and RT-qPCR

Total RNA was purified using Quick-RNA miniprep Kit. Reverse transcription was carried out using iScript Reverse Transcription Supermix. qPCR was performed using Bimake SYBR Green qPCR Master Mix with the following primers:

1060 (SARS-S Forward): GTTCAAGGACGGCATCTACTT
1061 (SARS-S Reverse): ACGCTCTGGGACTTGTTATTC
1062 (SARS2-S Forward): GACAAAGTGCACCCTGAAGA
1063 (SARS2-S Reverse): GGGCACAGGTTGGTGATATT
1089 (MERS-S Forward): GAACGCCTCTCTGAACTCTTT

1090 (MERS-S Reverse): GTCCTCGGTGATGTTGTATGT

1091 (F1 and F2 Forward): GATTAGAGCCGCCGAGATTAG

1092 (F1 and F2 Reverse): GGACTGAGGGAAAGACATGAG

Since the synthesized genes of F1 and F2 were optimized for mammalian expression and different from the gene coding for SARS2-S, the qPCR primers 1091 and 1092 were unique to F1 and F2, while 1062 and 1063 were unique to SARS2-S.

Minicircle production

F1-coding gene was cloned into the minicircle parental vector pMC.CMV-MCS-SV40polyA (MN501A) to yield MN501A-F1. MN501A or MN501A-F1 was transformed into ZYCY10P3S2T *E. coli* minicircle producer strain competent cells following the manufacturer's instruction. The production of minicircle DNA was induced with the addition of Arabinose Induction Solution. Minicircle DNA was purified by using ZymoPURE II Plasmid Maxiprep Kit per the manufacturer's instruction.

Pseudovirus generation, precipitation and concentration

Pseudovirus generation followed the protocol reported earlier[25]. Essentially, HEK293T cells were seeded on 6-well plates the night before. The next day, pcDNA3.1-SARS2-S (0.6 μg) and pRL4.3-Luc-R^-E^- (0.6 μg) were used to transfect one-well HEK293T cells using Lipofectine 3000. MN501A minicircle or F1 minicircle at indicated molar ratio was included in the transfection mixture. At 16 hours post-transfection, the HEK293T cells were fed with fresh medium. At 48 hours after medium change, the supernatant of each well of the 6-well plates was harvested, and centrifuged at 300 g for 5 minutes to remove cell debris. Pseudoviruses were purified using QuickTiter Lentivirus Titer kit following the manufacturer's instruction. The virus lysate was analyzed by western blot using rhodopsin antibody 1D4 HRP for spike proteins, and FITC-conjugated anti-p24 mAb and HRP-

conjugated anti-FITC mAb for p24, which served as an internal control. A portion of pseudovirus-containing supernatant was concentrated by PEG8000 and used for luciferase assay of cell entry.

Luciferase assay of cell entry by pseudoviruses

HEK293T cells were seeded on 100 mm dishes the night before. The next day, HEK293T cells were transfected with 10 μg pcDNA3.1-hACE2 using Lipofectine 3000. At 16 hours post-transfection, the cells were resuspended in FBS-free DMEM medium, and plated onto 96-well white plates to which 10 μL concentrated pseudoviruses was already added to each well. Two hours later, each well was added with an equal volume of DMEM containing 20% FBS. The cells were further incubated for 36 hours, then an equal volume of One-Glo EX Luciferase Assay Reagent was added, after incubation for 3 minutes, the luminescence signals were recorded.

FRET between SARS2C and F1Y

High quality/high resolution automated imaging was performed on a GE Healthcare DVLive epifluorescence image restoration microscope using an Olympus PlanApoN 60X/1.42 NA objective and a 1.9k x 1.9k pco.EDGE sCMOS_5.5 camera with a 1024x1024 FOV. The filter sets used were: CFP (438/24 excitation, 470/24 emission) and YFP (513/17 excitation, 559/38 emission). Donor and Acceptor control channels were acquired using CFP-CFP and YFP-YFP, respectively. FRET images were acquired using CFP-YFP excitation and emission filter pair. Cells were chosen with similar intensity profiles in donor and acceptor prior to acquisition while under 37°C and 5% CO_2 environmental conditions. Z stacks (0.25μm) covering the whole cell (~12μm) were acquired before applying a conservative restorative algorithm for quantitative image deconvolution using SoftWorx v7.0, and saving files as a max pixel intensity projection tiff for each individual channel. The FRET ratio (FR)

was determined by using the three-cube approach[21] that was defined as the ratio of YFP emission in the presence of FRET over that in the absence of FRET:

$$FR=F_{A(D)}/\ F_A=[S_{FRET(DA)}-R_{D1}\bullet S_{CFP(DA)}]/R_{A1}\bullet[S_{YFP(DA)}-R_{D2}\bullet S_{CFP(DA)}]$$

Where $R_{D1}= S_{FRET(D)}/S_{CFP(D)}$; $R_{D2}=S_{YFP(D)}/S_{CFP(D)}$; $R_{A1}=S_{FRET(A)}/S_{YFP(A)}$; and S_{FRET}, S_{CFP} and S_{YFP} with D, A, DA in parenthesis refer to fluorescence signals of the FRET, CFP or YFP channel when only SARS2C (containing CFP as donor (D)), F1Y (containing YFP as acceptor (A)), or both SARS2C and F1Y-containing plasmids (both donor and acceptor (DA)) were included in the transfection. Averages from untransfected cells were subtracted from same-day fluorescence values for each filter cube. According to the definition, FR=1.0 means no FRET, while FR>1.0 indicates the presence of FRET between the proteins carrying donor and acceptor proteins.

Acknowledgements

J.M. acknowledges support from the Welch Foundation (Q-1512). Q.W. thanks support from the Welch Foundation (Q-1826). A.A.C was partially supported by a postdoctoral training fellowship from the Computational Cancer Biology Training Program of the Gulf Coast Consortia (CPRIT Grant No. RP170593). Imaging for this project was supported by the Integrated Microscopy Core at Baylor College of Medicine with funding from NIH (DK56338, and CA125123), CPRIT (RP150578, RP170719), the Dan L. Duncan Comprehensive Cancer Center, and the John S. Dunn Gulf Coast Consortium for Chemical Genomics. The authors thank Hannah Johnson and Dr. Fabio Stossi at Integrated Microscopy Core at Baylor College of Medicine for their help with collecting the FRET data.

Author contributions

J.M. and Q.W. conceptualized the project; J.M. and Q.W. developed the methodology; J.M., A.A.C. and Q.W. performed the investigations; J.M. and Q.W. wrote the original draft; J.M., A.A.C. and Q.W. reviewed and edited the paper.

Competing interests

A U.S. Provisional Patent (Application No. 63/168,107) has been filed on the method of polypeptide-based protein interference and on the anti-viral inhibitors (inventors: J.M. and Q.W.). A.A.C. declares no competing interest.

References

1 Cui, J., Li, F. & Shi, Z. L. Origin and evolution of pathogenic coronaviruses. *Nature reviews. Microbiology* **17**, 181-192, doi:10.1038/s41579-018-0118-9 (2019).

2 de Wit, E., van Doremalen, N., Falzarano, D. & Munster, V. J. SARS and MERS: recent insights into emerging coronaviruses. *Nature reviews. Microbiology* **14**, 523-534, doi:10.1038/nrmicro.2016.81 (2016).

3 Rambaut, A. *et al.* Preliminary genomic characterisation of an emergent SARS-CoV-2 lineage in the UK defined by a novel set of spike mutations. (2020).

4 Tegally, H., Wilkinson, E. & al., e. Emergence and rapid spread of a new severe acute respiratory syndrome-related coronavirus 2 (SARS-CoV-2) lineage with multiple spike mutations in South Africa. *medRxiv* **2020.2012.2021.20248640** (2020).

5 Naveca, F. *et al.* Phylogenetic relationship of SARS□CoV□2 sequences from Amazonas with emerging Brazilian variants harboring mutations E484K and N501Y in the Spike protein. *virological.org* (2021).

6 Zhou, D., Dejnirattisai, W., Supasa, P., Liu, C. & al., e. Evidence of escape of SARS-CoV-2 variant B.1.351 from natural and vaccine induced sera. *Cell* **In press** (2021).

7 Tada, T. *et al.* Neutralization of viruses with European, South African, and United States SARS-CoV-2 variant spike proteins by convalescent sera and BNT162b2 mRNA vaccine-elicited antibodies. *bioRxiv*, doi:10.1101/2021.02.05.430003 (2021).

8 Wang, P. *et al.* Increased Resistance of SARS-CoV-2 Variants B.1.351 and B.1.1.7 to Antibody Neutralization. *bioRxiv*, doi:10.1101/2021.01.25.428137 (2021).

9 Zhou, B. *et al.* SARS-CoV-2 spike D614G change enhances replication and transmission. *Nature*, doi:10.1038/s41586-021-03361-1 (2021).

10 Cele, S. *et al.* Escape of SARS-CoV-2 501Y.V2 from neutralization by convalescent plasma. *Nature*, doi:10.1038/s41586-021-03471-w (2021).

11 V'Kovski, P., Kratzel, A., Steiner, S., Stalder, H. & Thiel, V. Coronavirus biology and replication: implications for SARS-CoV-2. *Nature reviews. Microbiology* **19**, 155-170, doi:10.1038/s41579-020-00468-6 (2021).

12 Wrapp, D. *et al.* Cryo-EM structure of the 2019-nCoV spike in the prefusion conformation. *Science* **367**, 1260-1263, doi:10.1126/science.abb2507 (2020).
13 Walls, A. C. *et al.* Structure, Function, and Antigenicity of the SARS-CoV-2 Spike Glycoprotein. *Cell* **183**, 1735, doi:10.1016/j.cell.2020.11.032 (2020).
14 Shang, J. *et al.* Structural basis of receptor recognition by SARS-CoV-2. *Nature* **581**, 221-224, doi:10.1038/s41586-020-2179-y (2020).
15 Cai, Y. *et al.* Distinct conformational states of SARS-CoV-2 spike protein. *Science* **369**, 1586-1592, doi:10.1126/science.abd4251 (2020).
16 Bangaru, S. *et al.* Structural analysis of full-length SARS-CoV-2 spike protein from an advanced vaccine candidate. *Science* **370**, 1089-1094, doi:10.1126/science.abe1502 (2020).
17 Klein, S. *et al.* SARS-CoV-2 structure and replication characterized by in situ cryo-electron tomography. *Nat Commun* **11**, 5885, doi:10.1038/s41467-020-19619-7 (2020).
18 Stertz, S. *et al.* The intracellular sites of early replication and budding of SARS-coronavirus. *Virology* **361**, 304-315, doi:10.1016/j.virol.2006.11.027 (2007).
19 Coutard, B. *et al.* The spike glycoprotein of the new coronavirus 2019-nCoV contains a furin-like cleavage site absent in CoV of the same clade. *Antiviral Res* **176**, 104742, doi:10.1016/j.antiviral.2020.104742 (2020).
20 Johnson, B. A. *et al.* Loss of furin cleavage site attenuates SARS-CoV-2 pathogenesis. *Nature* **591**, 293-299, doi:10.1038/s41586-021-03237-4 (2021).
21 Erickson, M. G., Alseikhan, B. A., Peterson, B. Z. & Yue, D. T. Preassociation of calmodulin with voltage-gated Ca(2+) channels revealed by FRET in single living cells. *Neuron* **31**, 973-985, doi:10.1016/s0896-6273(01)00438-x (2001).
22 Hardee, C. L., Arevalo-Soliz, L. M., Hornstein, B. D. & Zechiedrich, L. Advances in Non-Viral DNA Vectors for Gene Therapy. *Genes (Basel)* **8**, doi:10.3390/genes8020065 (2017).
23 Catanese, D. J., Jr., Fogg, J. M., Schrock, D. E., 2nd, Gilbert, B. E. & Zechiedrich, L. Supercoiled Minivector DNA resists shear forces associated with gene therapy delivery. *Gene Ther* **19**, 94-100, doi:10.1038/gt.2011.77 (2012).
24 Kay, M. A., He, C. Y. & Chen, Z. Y. A robust system for production of minicircle DNA vectors. *Nat Biotechnol* **28**, 1287-1289, doi:10.1038/nbt.1708 (2010).
25 Zhao, G. *et al.* A safe and convenient pseudovirus-based inhibition assay to detect neutralizing antibodies and screen for viral entry inhibitors against the novel human coronavirus MERS-CoV. *Virol J* **10**, 266, doi:10.1186/1743-422X-10-266 (2013).
26 Madeira, F. *et al.* The EMBL-EBI search and sequence analysis tools APIs in 2019. *Nucleic Acids Res* **47**, W636-W641, doi:10.1093/nar/gkz268 (2019).

Supplementary Information

Figure S1. Amino-acid sequences of F1 and F2 polypeptides used in this study. Single-letter codes were used for amino acids. The signal peptide sequences were highlighted in boldface at the N-terminus. FLAG-tags at the extreme C-terminus of each polypeptide were underlined.

Figure S2. Sequence alignments of coronavirus spike proteins. a). The alignment of SARS2-S (SARS2), SARS-S (SARS), and SARS-CoV-2 B.1.1.7 spike protein (B.1.1.7). **b).** The alignment of SARS2-S (SARS2) and MERS-S (MERS) proteins. In both panels, the range of residues included in the F1 polypeptide was highlighted in blue boxes. The cleavage site between S1 and S2 was shown by a red arrow. Multiple sequence alignments were performed using CLUSTAL Omega[26]. The sequences were: SARS2-S (GenBank accession number AFR58740.1), SARS-S (GenBank accession number QHD43416.1), SARS-CoV-2 B.1.1.7-S (GenBank accession number QQH18545.1), and MERS-S (GenBank accession number QBM11748.1).

Figure S3. Sequence conservation of representative human coronavirus spike proteins comparing to SARS2-S. a). The comparison of SARS-S, B.1.1.7-S and MERS-S proteins with full-length SARS2-S. **b).** The comparison of representative human coronavirus spike proteins with SARS2-S F1 polypeptide (residues 911~1273). In both panels, shown were the number of residues that were identical (Identity), similar (Positive) and unmatched (Gap) comparing to SARS2-S, the total residues compared (after "/") and the corresponding percentage (in parenthesis). The total residues varied due to gaps in sequence alignments. The sequences were: SARS2-S (GenBank accession number AFR58740.1), SARS-S (GenBank accession number QHD43416.1), SARS-CoV-2 B.1.1.7-S (GenBank accession number QQH18545.1), MERS-S (GenBank accession number QBM11748.1), HCoV-HKU1-S (Uniprot

accession number Q0ZME7), HCoV-OC43-S (Uniprot accession number P36334), HCoV-NL63-S (Uniprot accession number Q6Q1S2), and HCoV-229E-S (Uniprot accession number P15423).

Figure S4. Protein expression levels of F1 and F2 when co-transfected with coronavirus spike protein-coding plasmids. a). with COVID-19 SARS2-S; **b).** with 2002 SARS-S; **c).** with 2012 MERS-S.

Figure S5. F1 interfered with coronavirus spike proteins at the protein level. a~c). The mRNA levels of spike proteins in the absence or presence of F1-carrying plasmid. **a).** COVID-19 SARS2-S; **b).** 2002 SARS-S; **c).** 2012 MERS-S. **d).** Diagram for the FRET setup, where CFP and YFP were each tagged to the extreme C-terminus of SARS2-S and F1, resulting in SARS2C and F1Y, respectively. **e).** FRET ratio of SARS2C with F1Y (at a 1:1 molar ratio for transfection), compared to that of F1Y only. ****, $p<0.0001$ in unpaired *t*-test comparing FRET ratios of SARS2C+F1Y *versus* same-day F1Y only. Numbers in parentheses indicate the number of cells included in each analysis.

Figure S6. The mRNA levels of F1 and F2 when co-transfected with coronavirus spike protein-coding plasmids. a). with COVID-19 SARS2-S; **b).** with 2002 SARS-S; **c).** with 2012 MERS-S.

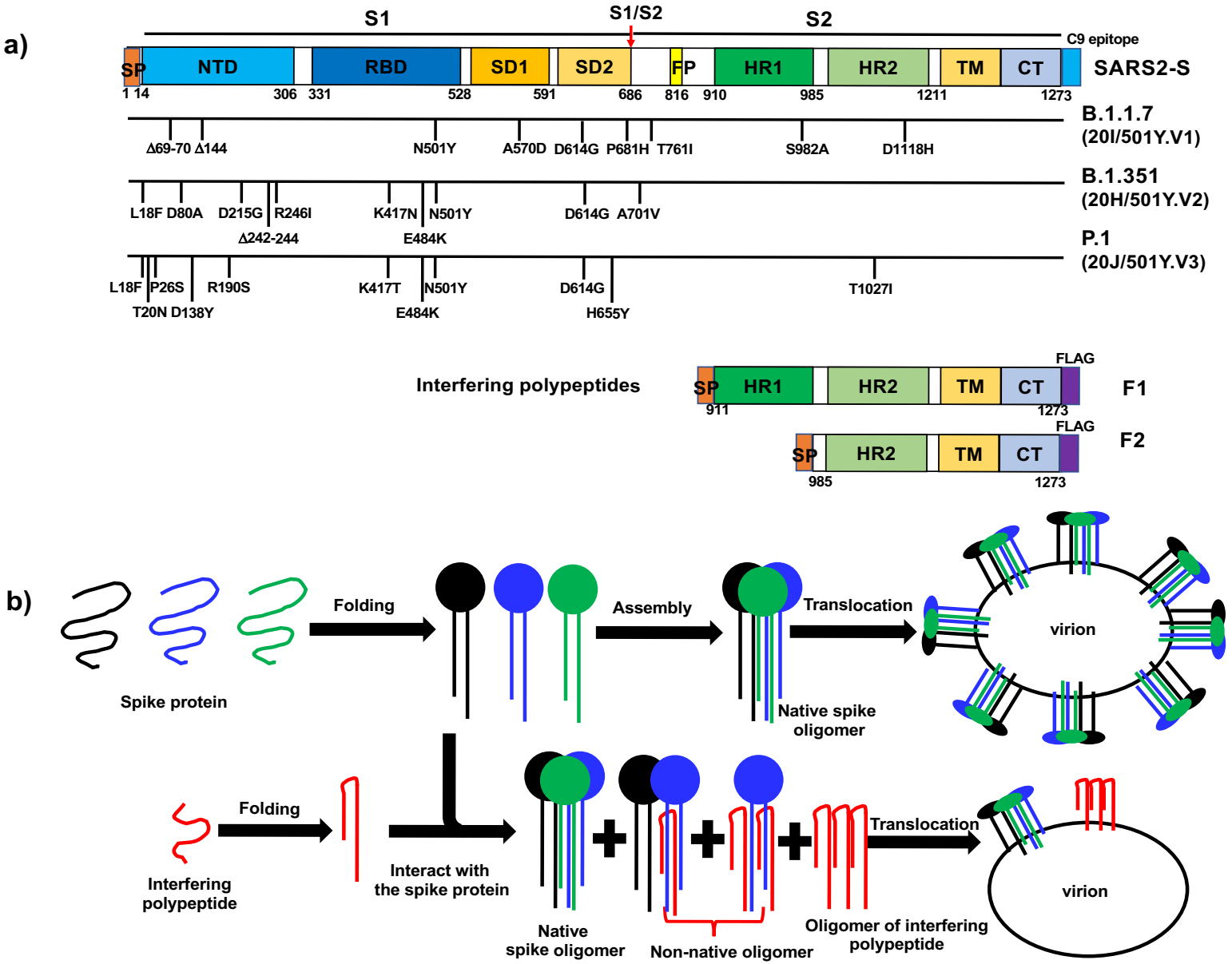

Figure 1. The concept of polypeptide-based protein interference against coronavirus spike proteins. a). Domain organization of COVID-19 SARS2-S, the mutations in recent variants and the design of interfering polypeptides F1 and F2. SP: Signal peptide; NTD: N-terminal domain; RBD: receptor-binding domain; SD1: subdomain 1; SD2: subdomain 2; FP: fusion peptide; HR1: heptad repeat 1; HR2: heptad repeat 2; TM: transmembrane domain; CT: Cytoplasmic tail. The cleavage at S1/S2 (red arrow) gives rise to N-terminal S1 fragment and C-terminal S2 fragment. The signal peptide sequence at the extreme N-termini of F1 and F2 allowed the polypeptides to be translocated in the same way as COVID-19 SARS2-S. At the extreme C-termini, SARS2-S had a C9 epitope recognized by C9-rhodopsin antibody 1D4, while both F1 and F2 had a FLAG-tag. **b).** Diagram of polypeptide-based interference targeting coronavirus spike proteins. Top row: in the normal situation, the spike proteins were synthesized, folded and formed native spike oligomers, which were anchored on virion envelope. Bottom row, interfering polypeptides formed non-native oligomers with the wild-type spike proteins, thus reducing the level of native spike oligomers on the envelope of new virions.

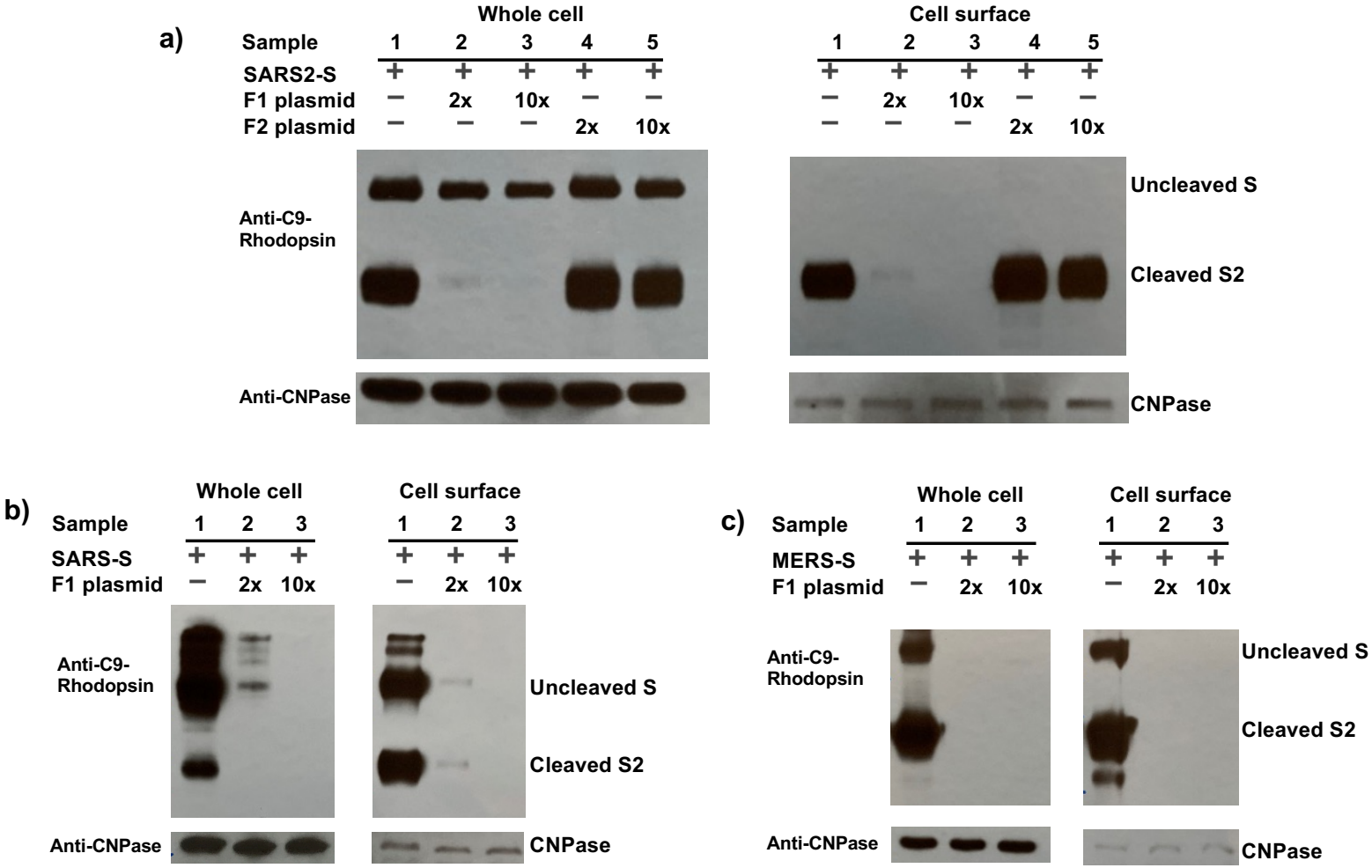

Figure 2. F1 significantly reduced expression and surface translocation of three coronavirus spike glycoproteins. **a).** COVID-19 SARS2-S. **b).** 2002 SARS-S. **c).** 2012 MERS-S. For panels **a-c)**, the levels of S protein in whole-cell lysate (left) or in cell-surface fraction (right) were compared for HEK293T cells transfected with S-containing plasmid only (Sample 1), or together with twofold (Sample 2) or tenfold molar ratio (Sample 3) of F1-containing plasmid, and in panel **a)** with twofold (Sample 4) or tenfold molar ratio (Sample 5) of F2-containing plasmid.

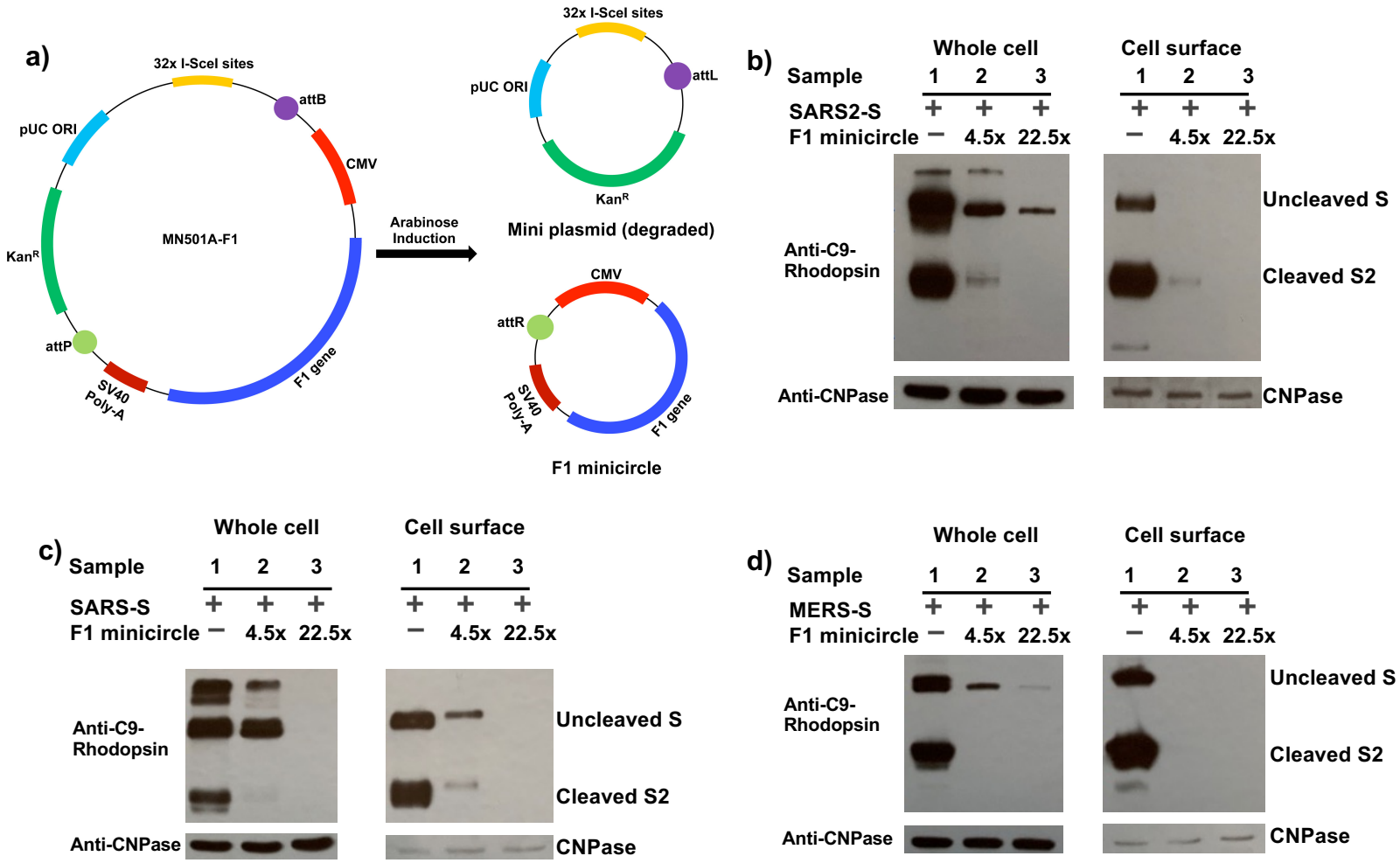

Figure 3. F1 minicircle significantly reduced expression and surface translocation of three coronavirus spike glycoproteins. a). Diagram for the production of F1 minicircle used in this study. **b).** COVID-19 SARS2-S; **c).** 2002 SARS-S; **d).** 2012 MERS-S. The levels of uncleaved S protein and the cleaved S2 protein in whole-cell lysate (left) or in cell-surface fraction (right) were compared for HEK293T cells transfected with S-containing plasmid only (Sample 1), or together with 4.5-fold (Sample 2) or 22.5-fold molar ratio (Sample 3) of F1 minicircles.

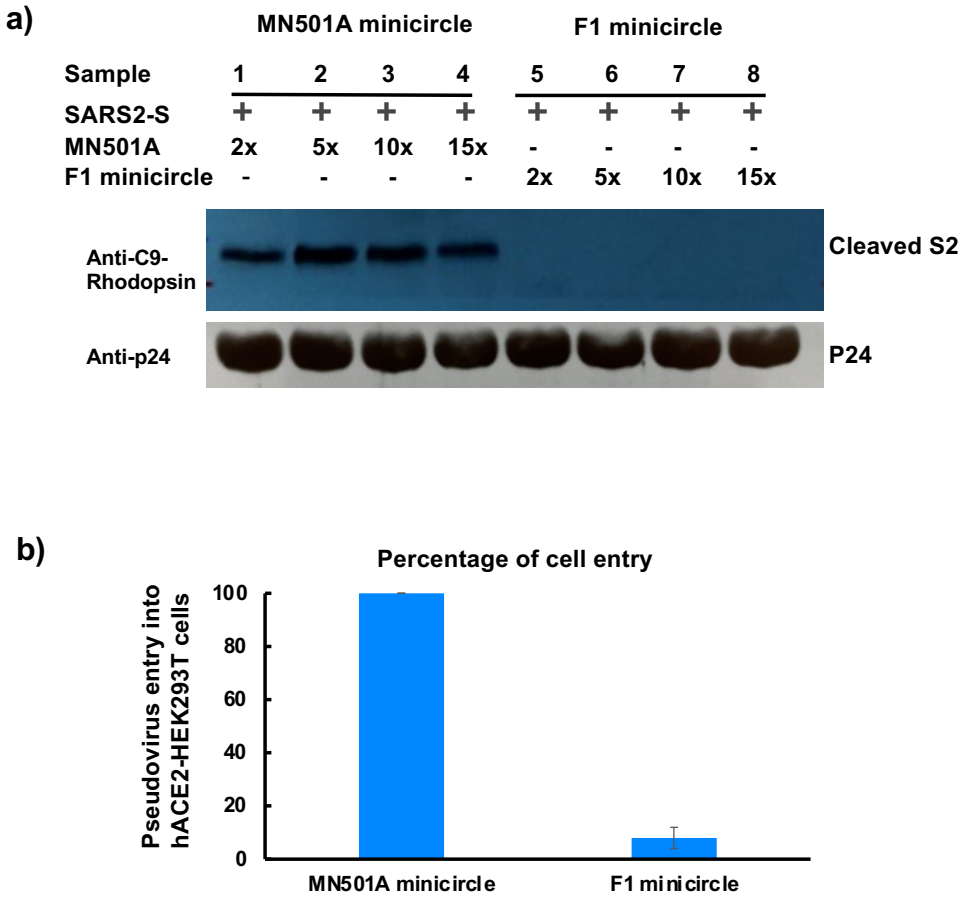

Figure 4. F1 minicircle significantly reduced the level of SARS2-S on intact pseudoviruses and impaired pseudovirus infectivity. a). The level of cleaved S2 protein was compared for intact pseudovirus produced from HEK293T cells transfected with SARS2-S-containing plasmid and different ratios of empty minicircle control, MN501A (Sample 1~4), or F1 minicircle (Sample 5~8). **b).** Pseudovirus generated in the presence of only twofold molar ratio of F1 minicircle completely lost the ability to infect hACE2-expressing HEK293T cells. The infectivity of pseudovirus generated in the presence of twofold molar ratio of MN501A minicircle was considered as 100%.

F1:

MFVFLVLLPLVSSQCVNLTTRTQVTQNVLYENQKLIANQFNSAIGKIQDSLSSTASALGKLQDVVNQNAQ
ALNTLVKQLSSNFGAISSVLNDILSRLDKVEAEVQIDRLITGRLQSLQTYVTQQLIRAAEIRASANLAAT
KMSECVLGQSKRVDFCGKGYHLMSFPQSAPHGVVFLHVTYVPAQEKNFTTAPAICHDGKAHFPREGVFVS
NGTHWFVTQRNFYEPQIITTDNTFVSGNCDVVIGIVNNTVYDPLQPELDSFKEELDKYFKNHTSPDVDLG
DISGINASVVNIQKEIDRLNEVAKNLNESLIDLQELGKYEQYIKWPWYIWLGFIAGLIAIVMVTIMLCCM
TSCCSCLKGCCSCGSCCKFDEDDSEPVLKGVKLHYTDYKDDDDK

F2:

MFVFLVLLPLVSSQCVNLTTRTQDKVEAEVQIDRLITGRLQSLQTYVTQQLIRAAEIRASANLAATKMSE
CVLGQSKRVDFCGKGYHLMSFPQSAPHGVVFLHVTYVPAQEKNFTTAPAICHDGKAHFPREGVFVSNGTH
WFVTQRNFYEPQIITTDNTFVSGNCDVVIGIVNNTVYDPLQPELDSFKEELDKYFKNHTSPDVDLGDISG
INASVVNIQKEIDRLNEVAKNLNESLIDLQELGKYEQYIKWPWYIWLGFIAGLIAIVMVTIMLCCMTSCC
SCLKGCCSCGSCCKFDEDDSEPVLKGVKLHYTDYKDDDDK

Figure S1. Amino-acid sequences of F1 and F2 polypeptides used in this study. Single-letter codes were used for amino acids. The signal peptide sequences were highlighted in boldface at the N-terminus. FLAG-tags at the extreme C-terminus of each polypeptide were underlined.

a)

Figure S2. Sequence alignments of coronavirus spike proteins. a). The alignment of SARS2-S (SARS2), SARS-S (SARS), and SARS-CoV-2 B.1.1.7 spike protein (B.1.1.7). **b).** The alignment of SARS2-S (SARS2) and MERS-S (MERS) proteins. In both panels, the range of residues included in the F1 polypeptide was highlighted in blue boxes. The cleavage site between S1 and S2 was shown by a red arrow. Multiple sequence alignments were performed using CLUSTAL Omega[24]. The sequences were: SARS2-S (GenBank accession number AFR58740.1), SARS-S (GenBank accession number QHD43416.1), SARS-CoV-2 B.1.1.7-S (GenBank accession number QQH18545.1), and MERS-S (GenBank accession number QBM11748.1).

b)

Figure S2. Sequence alignments of coronavirus spike proteins. a). The alignment of SARS2-S (SARS2), SARS-S (SARS), and SARS-CoV-2 B.1.1.7 spike protein (B.1.1.7). **b).** The alignment of SARS2-S (SARS2) and MERS-S (MERS) proteins. In both panels, the range of residues included in the F1 polypeptide was highlighted in blue boxes. The cleavage site between S1 and S2 was shown by a red arrow. Multiple sequence alignments were performed using CLUSTAL Omega[24]. The sequences were: SARS2-S (GenBank accession number AFR58740.1), SARS-S (GenBank accession number QHD43416.1), SARS-CoV-2 B.1.1.7-S (GenBank accession number QQH18545.1), and MERS-S (GenBank accession number QBM11748.1).

a)

	With SARS2-S (1~1273)		
Spike protein	**Identity**	**Positive**	**Gap**
SARS-S	963/1250 (77%)	1097/1250 (87%)	24/1250 (1%)
B.1.1.7-S	1263/1273 (99%)	1264/1273 (99%)	3/1273 (0%)
MERS-S	370/1057 (35%)	545/1057 (51%)	76/1057 (7%)

b)

	With SARS2-S F1 (911~1273)		
Spike protein	**Identity**	**Positive**	**Gap**
SARS-S (*Betacoronavirus*, lineage B)	340/363 (94%)	356/363 (98%)	0/363 (0%)
B.1.1.7-S (*Betacoronavirus*, lineage B)	361/363 (99%)	362/363 (99%)	0/363 (0%)
MERS-S (*Betacoronavirus*, lineage C)	156/368 (42%)	219/368 (59%)	20/363 (5%)
HCoV-HKU1-S (*Betacoronavirus*, lineage A)	154/347 (44%)	218/347 (62%)	12/347 (3%)
HCoV-OC43-S (*Betacoronavirus*, lineage A)	160/358 (45%)	224/358 (62%)	6/358 (1%)
HCoV-NL63-S (*Alphacoronavirus*)	136/386 (35%)	202/386 (52%)	56/386 (14%)
HCoV-229E-S (*Alphacoronavirus*)	135/377 (36%)	201/377 (53%)	46/377 (12%)

Figure S3. Sequence conservation of representative human and bat coronavirus spike proteins comparing to SARS2-S. a). The comparison of SARS-S, B.1.1.7-S and MERS-S proteins with full-length SARS2-S. **b).** The comparison of representative human and bat coronavirus spike proteins with SARS2-S F1 polypeptide (residues 911~1273). In both panels, shown were the number of residues that were identical (Identity), similar (Positive) and unmatched (Gap) comparing to SARS2-S, the total residues compared (after "/") and the corresponding percentage (in parenthesis). The total residues varied due to gaps during sequence alignments. The sequences were: SARS2-S (GenBank accession number AFR58740.1), SARS-S (GenBank accession number QHD43416.1), SARS-CoV-2 B.1.1.7-S (GenBank accession number QQH18545.1), MERS-S (GenBank accession number QBM11748.1), HCoV-HKU1-S (Uniprot accession number Q0ZME7), HCoV-OC43-S (Uniprot accession number P36334), HCoV-NL63-S (Uniprot accession number Q6Q1S2), and HCoV-229E-S (Uniprot accession number P15423).

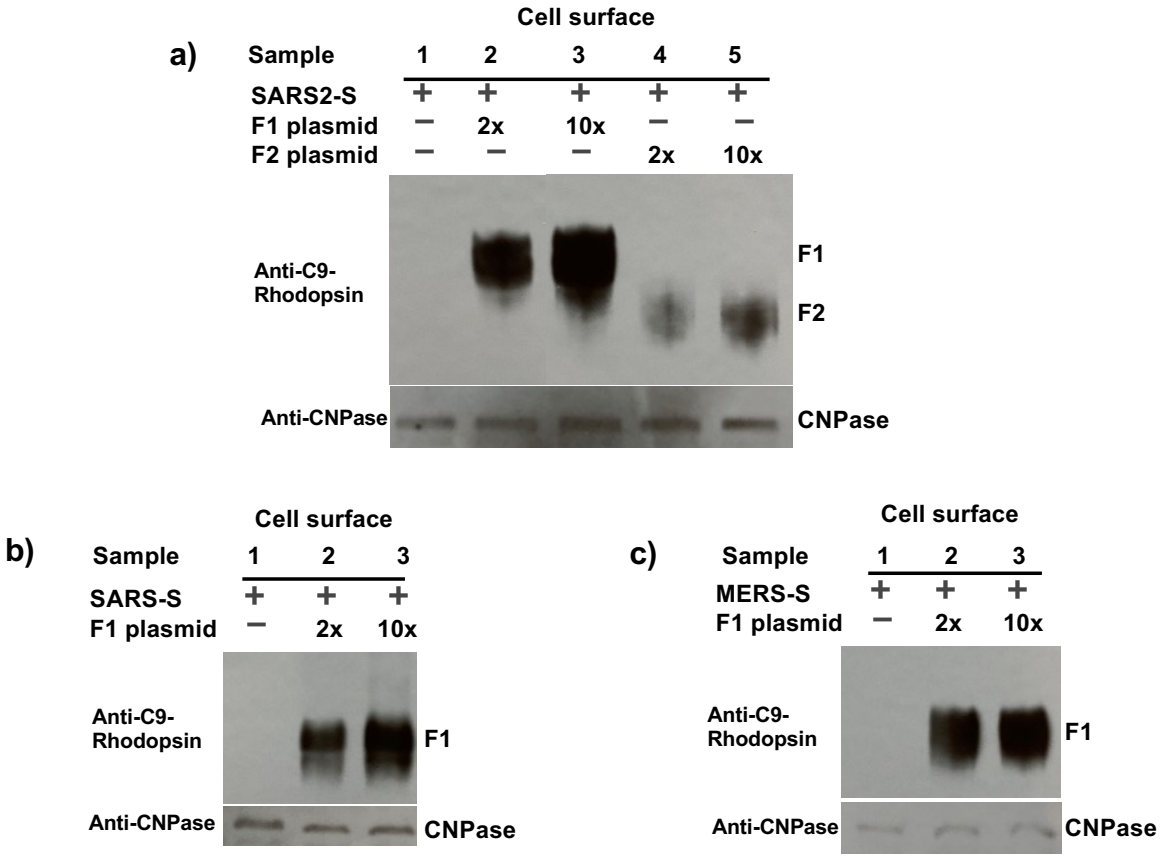

Figure S4. Protein expression levels of F1 and F2 when co-transfected with coronavirus spike protein-coding plasmids. a). with COVID-19 SARS2-S; **b).** with 2002 SARS-S; **c).** with 2012 MERS-S.

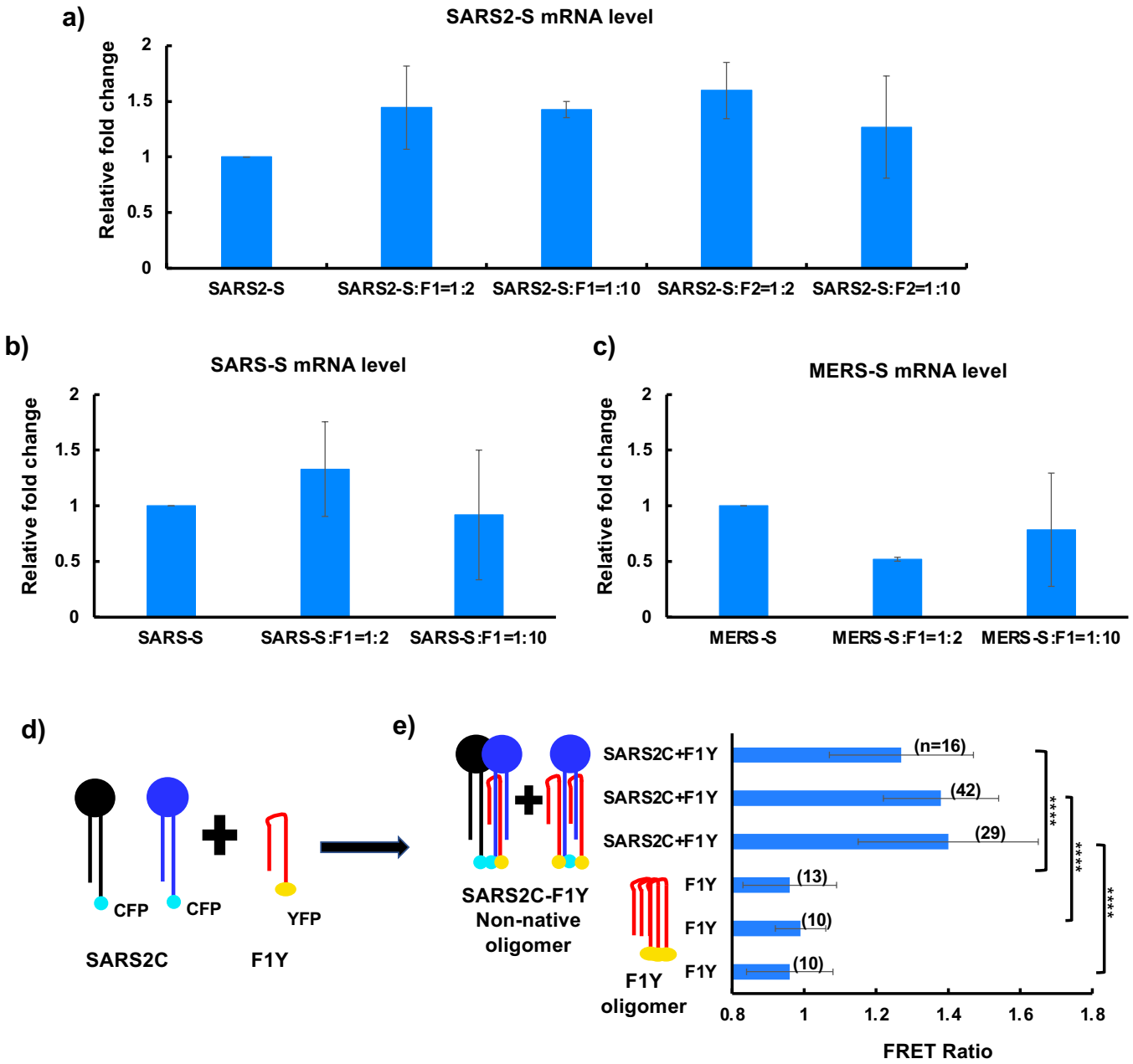

Figure S5. F1 interfered with coronavirus spike proteins at the protein level. a~c). The mRNA levels of spike proteins in the absence or presence of F1-carrying plasmid. **a).** COVID-19 SARS2-S; **b).** 2002 SARS-S; **c).** 2012 MERS-S. **d).** Diagram for the FRET setup, where CFP and YFP were each tagged to the extreme C-terminus of SARS2-S and F1, resulting in SARS2C and F1Y, respectively. **e).** FRET ratio of SARS2C with F1Y (at a 1:1 molar ratio for transfection), compared to that of F1Y only. ****, p<0.0001 in unpaired t-test comparing FRET ratios of SARS2C+F1Y *versus* same-day F1Y only. Numbers in parentheses indicate the number of cells included in each analysis.

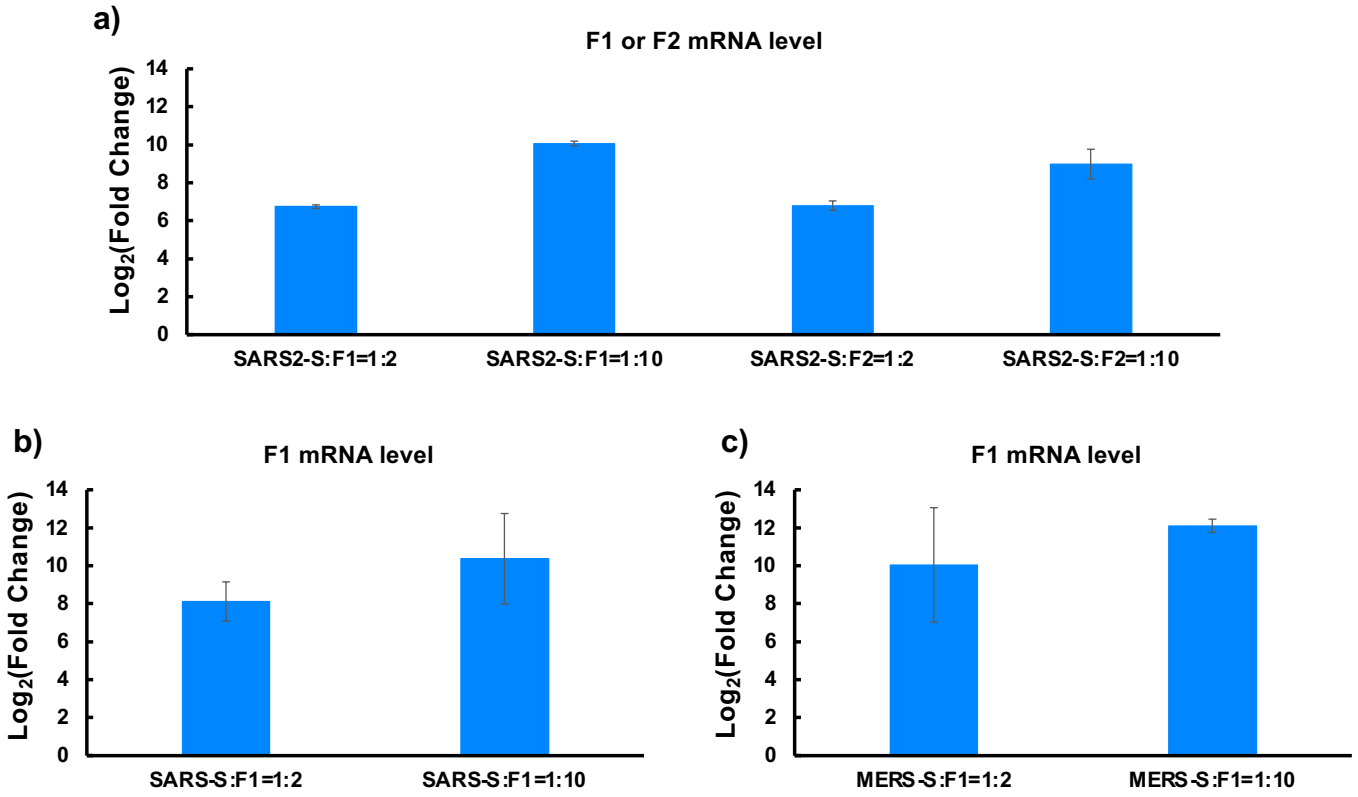

Figure S6. The mRNA levels of F1 and F2 when co-transfected with coronavirus spike protein-coding plasmids.
a). with COVID-19 SARS2-S; **b).** with 2002 SARS-S; **c).** with 2012 MERS-S.